Molecular Pharmacology Fast Forward. Published on April 5, 2010 as doi: 10.1124/mol.109.061101

Pravastatin Attenuates Carboplatin-Induced Nephrotoxicity in Rodents via Peroxisome Proliferator-Activated Receptor Alpha–Regulated Heme Oxygenase-1

Hsi-Hsien Chen, Tzen-Wen Chen, Heng Lin

Graduate Institute of Clinical Medicine, College of Medicine, Taipei Medical University, Taipei, Taiwan (H-H.C., T-W.C); Department of Internal Medicine, Taipei Medical University Hospital, Taipei, Taiwan (H-H.C., T-W.C); Graduate Institute of Pharmacology and Toxicology, Tzu Chi University, Hualien, Taiwan (H.L.)

Molecular Pharmacology Fast Forward. Published on April 5, 2010 as DOI: 10.1124/mol.109.061101
This article has not been copyedited and formatted. The final version may differ from this version.

Running title: Pravastatin-Induced Decrease in Carboplatin Nephrotoxicity

Address correspondence to: Heng Lin, Graduate Institute of Pharmacology and Toxicology, Tzu Chi University, No.701 Zhongyang Rd., Sec. 3, Hualien, 97004 Taiwan; Phone: 886-02-27899135; Fax: 886-02-27827654; e-mail address: linheng@ibms.sinica.edu.tw.

Number of text pages: 35 total manuscript pages/21 main text pages

Number of figures: 7 (plus 6 supplemental figures)

Number of tables: 0

Number of references: 30

Abstract: 198

Introduction: 531

Discussion: 1510

Nonstandard abbreviations: ChIP, chromatin immunoprecipitation; CM-H_2DCFDA, chloromethyl-2',7'-dichlorodihydrofluorescein diacetate; COX-2, cyclooxygenase-2; DCF, dichlorodihydrofluorescein; HMG-CoA, 3-hydroxy-3-methylglutaryl-coenzyme A; HO-1, heme oxygenase-1; IL, interleukin; NO, nitric oxide; PGI_2, prostaglandin I_2; PPARα, peroxisome proliferator-activated receptor-α; PPRE, peroxisome proliferator response element; ROS, reactive oxygen species; siRNA, small interfering RNA; TUNEL, terminal deoxynucleotidyl transferase dUTP nick end labeling.

Molecular Pharmacology Fast Forward. Published on April 5, 2010 as DOI: 10.1124/mol.109.061101
This article has not been copyedited and formatted. The final version may differ from this version.

ABSTRACT

The aim of this study was to explore the molecular mechanisms underlying the protective effect of pravastatin against carboplatin-induced nephrotoxicity in rodents. We exposed rat NRK-52E renal tubular epithelial cells to carboplatin, with or without pravastatin. Pravastatin decreased production of reactive oxygen species (ROS), increased expression of heme oxygenase-1 (HO-1), cyclooxygenase-2 (COX-2), and 6-keto prostaglandin (PG) F1α, enhanced nuclear translocation of peroxisome proliferator-activated receptor-α (PPARα), and increased HO-1 promoter and peroxisome proliferator response element (PPRE) activities. We found interaction of PPARα with PPRE on the HO-1 promoter in nuclear extracts from pravastatin-treated NRK-52E cells and by chromatin immunoprecipitation. We pretreated mice with pravastatin and then administered a single intraperitoneal injection of carboplatin. Effects on renal function, morphology, apoptosis, and survival were assessed. In response to carboplatin injection, mice developed acute renal failure, with elevated activated caspase-3, increased apoptotic bodies, and decreased survival. Pretreatment with pravastatin significantly ameliorated renal dysfunction and apoptosis and improved renal morphology and survival. Injection of pravastatin also induced overexpression of PPARα and HO-1 in wild-type mice, and HO-1 expression was significantly attenuated in PPARα-knockout mice. These results indicate that pravastatin upregulates HO-1 and protects against carboplatin-induced renal dysfunction and apoptosis via a PPARα-dependent pathway.

Molecular Pharmacology Fast Forward. Published on April 5, 2010 as DOI: 10.1124/mol.109.061101
This article has not been copyedited and formatted. The final version may differ from this version.

Carboplatin (cis-diammine-1,1-cyclobutane dicarboxylate platinum II), a second-generation, platinum-containing, anticancer drug, is currently used in the treatment of lung and ovarian cancers, as well as head and neck cancers (Fujiwara et al., 2003; Pivot et al., 2001). Because carboplatin has fewer toxic effects than cisplatin, it can be used at higher doses to achieve optimal antitumor effects (reviewed by Alberts, 1995). However, its byproduct, platinum-ammine-DNA adduct, accumulates in the kidney and induces renal tubular damage (reviewed by Kintzel, 2001); this limits its use.

3-Hydroxy-3-methylglutaryl-coenzyme A (HMG-CoA) reductase inhibitors (statins) are lipid-lowering agents that are widely used in medical practice to lower plasma levels of low-density lipoprotein cholesterol. It is generally accepted that mechanisms beyond the reduction of plasma cholesterol contribute significantly to the anti-atherogenic and tissue-protective properties of statins (reviewed by Takemoto and Liao, 2001). Cholesterol-independent effects of statins include indirect anti-inflammatory effects such as activation of reduction-oxidation reaction (redox)–sensitive transcription factors (Gueler et al., 2002). Statins also protect tissues from various types of insults such as ischemia-reperfusion injury in the kidney and heart (Gueler et al., 2007; Birnbaum et al., 2005; Li, Yang et al., 2004; Cheng et al., 2008).

Some studies have demonstrated that statins lead to activation of the promoter for the antioxidant defense protein heme oxygenase-1 (HO-1), along with its transcription and

Molecular Pharmacology Fast Forward. Published on April 5, 2010 as DOI: 10.1124/mol.109.061101
This article has not been copyedited and formatted. The final version may differ from this version.

accumulation (Lee et al., 2004), which may help to explain the pleiotropic antioxidant and anti-inflammatory actions of statins (Grosser et al., 2004). Heme oxygenase-1, an inducible enzyme that catabolizes heme to biliverdin, ferrous iron, and carbon monoxide, exhibits cytoprotective effects against oxidative insults (reviewed by Sikorski et al., 2004). There are many HO-1 inducers including ultraviolet A radiation; hydrogen peroxide; cytokines (interleukin [IL]-1, IL-6, IL-10, tumor necrosis factor, interferon-γ); endotoxin; growth factors (platelet-derived growth factor, transforming growth factor-β); oxidized lipids; hyperoxia; nitric oxide (NO); NO donors; prostacyclin; peroxisome proliferator-activated receptor (PPAR) α and γ; angiotensin II; and glucose deprivation (reviewed by Ferrándiz and Devesa, 2008). Several of these stimuli play important roles in the pathophysiology of acute renal failure (Nath et al., 2001). Heme oxygenase-1 has been shown to be upregulated and to ameliorate the severity of renal damage in a variety of kidney injury models, such as kidney transplant rejection (Cuturi et al., 1999), and to inhibit the effects of nephrotoxins induced by cisplatin and cyclosporine (Agarwal et al., 1995; Li, Wu, et al., 2004).

Peroxisome proliferator-activated receptors are nuclear hormone receptors that form heterodimers with retinoid X receptors, which then activate or repress target genes. Li, Wu, and colleagues (2004) reported that pretreatment with Wy-14643, a ligand for PPARα, ameliorates cisplatin-induced acute renal failure on the basis of changes in blood urea nitrogen, creatinine, and tissue histology.

Molecular Pharmacology Fast Forward. Published on April 5, 2010 as DOI: 10.1124/mol.109.061101
This article has not been copyedited and formatted. The final version may differ from this version.

Whether statins can protect against carboplatin-induced renal injury via cholesterol-independent pathways is not clear. The effects of statins on PPARα are not completely defined, although another lipid-lowering agent, clofibrate, has been shown to be a ligand for PPARα (Forman et al., 1997). We hypothesized that the protective effects of statins against carboplatin-induced renal injury may be mediated by PPARα and HO-1. To test this hypothesis, we investigated the effects of pravastatin on PPARα and HO-1 in a rat renal epithelial cell line and in mouse models.

Materials and Methods

Animals and treatment with carboplatin and pravastatin. Male C57/B6, H129 wild-type, and H129 PPARα-knockout ($PPAR\alpha^{-/-}$) mice received humane care in compliance with the *Principles of Laboratory Animal Care* formulated by the National Society for Medical Research and the *Guide for the Care and Use of Laboratory Animals* prepared by the Institute of Laboratory Animal Resources (National Institutes of Health publication No. 86-23, revised 1985). The study protocol was approved by our institutional ethics committee on animal research. Pravastatin (Sigma-Aldrich, St. Louis, MO) was dissolved in double-distilled water, and carboplatin (Sigma-Aldrich) was dissolved in dimethyl sulfoxide (DMSO) just before use.

Ten-week-old mice were administered an intraperitoneal (i.p.) injection of a single

Molecular Pharmacology Fast Forward. Published on April 5, 2010 as DOI: 10.1124/mol.109.061101
This article has not been copyedited and formatted. The final version may differ from this version.

dose of carboplatin (100 mg/kg), with (experimental group) or without (control group) i.p. injection with pravastatin (5 mg/kg) (Sigma-Aldrich) 1 day before carboplatin treatment. The control group was treated with the same volume of normal saline (i.p.) instead of pravastatin.

Cell culture and transfection. The NRK-52E renal tubule epithelial cell line was obtained from American Type Culture Collection (ATCC, Manassas, VA) and cultured in Dulbecco modified Eagle medium supplemented with 10% fetal bovine serum, 100 units/ml penicillin, and 100 μg/ml streptomycin at 37°C in an atmosphere containing 5% CO_2, as described previously (Chen et al., 2009). Cells were transfected the following day with Lipofectamine (Invitrogen, Carlsbad, CA) containing 1.5 μg luciferase reporter plasmid and various amounts of PPARα, PPARα small interfering (si) RNA (5'CCCTTATCTGAAGAATTCTTA3'), or FLAG-PPARα expression vector per 6-cm^2 culture dish. The amount of DNA was kept constant with the use of empty expression vector. Cells were subjected to assays 16 to 24 h later.

Measurement of biochemical parameters and extraction of cytoplasmic and nuclear protein. Blood samples (500 μl) were collected from the tail vein. Samples were centrifuged (6000 g × 3 min) to separate the serum from the cells. Serum biochemical parameters were measured within 24 h of blood sampling.

For cytoplasmic and nuclear protein extraction, cells and kidney tissues were separated into nuclear and cytoplasmic fractions and extracted according to the manufacturer's protocol

Molecular Pharmacology Fast Forward. Published on April 5, 2010 as DOI: 10.1124/mol.109.061101
This article has not been copyedited and formatted. The final version may differ from this version.

(Pierce Chemical Company, Rockford, IL).

Terminal deoxynucleotidyl transferase dUTP nick end labeling. We detected DNA fragmentation in cells and animal tissues by labeling the termini of nucleic acids with the terminal deoxynucleotidyl transferase dUTP nick end labeling (TUNEL) method (Roche, Mannheim, Germany). Mice were perfused with 4% paraformaldehyde in 0.1 M phosphate buffer (pH 7.4). Organs were dissected, postfixed overnight in 4% paraformaldehyde, embedded in paraffin, and sectioned (5-μm thickness). The TUNEL assay was performed according to the manufacturer's protocol.

Nuclear extracts and electrophoretic mobility shift assays. For the peroxisome proliferator response element (PPRE) primer, we designed a PPARα DNA-binding sequence (5'-GAGTTGTAAGGTCATGGGAAA-3') for use in electrophoretic mobility shift assays. Electrophoretic mobility shift assay analysis of nuclear extracts was carried out as described previously (Lin et al., 2008). Binding reactions were performed in 20-μl reaction mixtures with 3 μg of nuclear extract in a buffer containing 12 mM HEPES (pH 7.9), 5 mM $MgCl_2$, 60 mM KCl, 4 mM Tris-HCl (pH 7.9), 0.6 mM ethylenediaminetetraacetic acid (EDTA), 0.6 mM dithiothreitol, 0.5 mg/ml bovine serum albumin, 1 μg poly[d(I-C)], 12% glycerol, and 20,000 cpm radiolabeled, double-stranded, 21-bp PPRE probe for 20 min at room temperature. Reactions were loaded onto a 4% polyacrylamide gel and run at 200 V at room temperature in 0.25× Tris/borate/EDTA buffer. The gel was dried and exposed to x-ray film

Molecular Pharmacology Fast Forward. Published on April 5, 2010 as DOI: 10.1124/mol.109.061101
This article has not been copyedited and formatted. The final version may differ from this version.

(Kodak, Rochester, NY).

Histopathologic preparations and immunocytochemistry. Kidneys from all of the treated groups were fixed in 10% buffered formalin overnight at 4°C and processed in paraffin wax. Sections (5-μm thickness) were stained with hematoxylin and eosin.

For immunocytochemistry, NRK-52E cells transfected with FLAG-PPARα plasmid were plated onto 35-mm poly-L-lysine–coated glass-bottomed dishes (Matsunami Glass Ind., Ltd., Osaka, Japan) and fixed for 20 min at room temperature in 4% paraformaldehyde and 0.4% Triton X-100 in phosphate-buffered saline (PBS). The cells were incubated with antibodies against FLAG (rabbit polyclonal; Sigma-Aldrich) in PBS containing 0.05% Tween 20 (PBST) plus 2% horse serum. After washing three times with PBS, the cells were incubated with Alexa 488-conjugated anti-rabbit IgG (Molecular Probes, Eugene, OR) and Cy3-conjugated anti-mouse IgG (Amersham Biosciences, Piscataway, NJ) in PBST containing 2% horse serum for 1 h at room temperature. Images were obtained with a fluorescence microscope.

Chromatin immunoprecipitation assay. NRK-52E cells were transfected with FLAG-PPARα plasmid 1 day after treatment with pravastatin, fixed in 1% formaldehyde, and chromatin immunoprecipitation (ChIP) assays were performed according to the manufacture's protocol (Millipore, Billerica, MA). Chromatin was immunoprecipitated with anti-FLAG antibody (Sigma-Aldrich) and anti-acetyl H4 antibody (Millipore). Purified DNA

Molecular Pharmacology Fast Forward. Published on April 5, 2010 as DOI: 10.1124/mol.109.061101
This article has not been copyedited and formatted. The final version may differ from this version.

was detected by standard polymerase chain reaction.

HO-1 promoter and PPRE reporter assay. The human HO-1-α promoter (positions –800 to +17) and three repeats of the PPRE-binding sequence were each cloned into pGL2-basic promoterless plasmid vectors (Promega, Madison, WI) and transfected into NRK-52E cells. Promoter-induced luciferase activity was measured as described previously (Chen et al., 2009).

Dichlorofluorescein assay for reactive oxygen species. The intracellular formation of reactive oxygen species (ROS) was detected with the fluorescent probe 5- (and 6-) chloromethyl-2',7'-dichlorodihydrofluorescein diacetate (CM-H_2DCFDA; Molecular Probes). NRK-52E cells (10^6 cells/ml) were cultured in the presence of 100 μM carboplatin for 24 h or pretreated for 30 min with 50 μM pravastatin and then loaded with 0.1 μg/ml CM-H_2DCFDA at 37°C for 30 min in the dark. Cells were then washed twice with Hank balanced salt solution (HBSS) containing calcium and magnesium. Dichlorodihydrofluorescein (DCF) fluorescence was measured immediately with a charge-couple device (CCD) camera (DP72, Olympus, Melville, NY) coupled to a microscope system (BX51, Olympus) at 100× magnification.

Statistical analysis. Continuous variables were compared by one-way analysis of variance (ANOVA). When there was a significant difference between groups, multiple comparisons of means were performed with the Bonferroni procedure and type-I error

Molecular Pharmacology Fast Forward. Published on April 5, 2010 as DOI: 10.1124/mol.109.061101
This article has not been copyedited and formatted. The final version may differ from this version.

adjustment. All statistical assessments were two-sided and evaluated at the 0.05 level of significance. Statistical analyses were performed with SPSS 15.0 statistics software (SPSS Inc., Chicago, IL). Survival analysis was performed according to the Kaplan-Meier method, and between-group differences in survival were tested by log-rank test.

Results

Carboplatin stimulated apoptosis and caspase activation in vitro and in vivo. To determine if carboplatin-induced nephrotoxicity occurred via a caspase-dependent pathway in vitro, NRK-52E renal epithelial cells were treated with increasing carboplatin concentrations (50–800 μM), which resulted in a concentration-dependent increase in the level of caspase-3 (Fig. 1A); this increase continued for at least 48 h (Fig. 1B). Treatment with the caspase inhibitor Z-VAD (Merck, Whitehouse Station, NJ) showed that carboplatin induced apoptosis in a caspase-dependent manner in Western blot and TUNEL assays (Supplemental Figs. 1 and 2). In addition, infection of NRK-52 cells with adenovirus containing HO-1 resulted in overexpression of HO-1 and a decrease in carboplatin-induced caspase-3 expression (Supplemental Fig. 3). To assay for possible iron toxicity induced by overexpression of HO-1, which can result in increased generation of ROS and inflammation, we overexpressed HO-1 by adenovirus infection in neuronal PC-12 cells (Supplemental Fig. 4). Results showed that overexpression of HO-1 induced ferric iron deposition, which was decreased by treatment

Molecular Pharmacology Fast Forward. Published on April 5, 2010 as DOI: 10.1124/mol.109.061101
This article has not been copyedited and formatted. The final version may differ from this version.

with the iron chelator deferoxamine. We also assayed PC-12 cell cytotoxicity and showed that overexpression of HO-1 induced more cytotoxicity in PC-12 cells than in NRK-52 cells, indicating that the effects of HO-1 may be tissue dependent.

We explored the effects of carboplatin in vivo by determining the expression of caspase-3 in kidney cells of mice injected with 100 mg/kg carboplatin. Immunoblotting results showed significantly increased staining for caspase-3 in the kidneys of carboplatin-treated mice (2 days after single treatment; Fig. 1C). Apoptosis in kidney cells of mice treated with carboplatin was also significantly ($p < 0.01$) increased to 16% compared to that of control mice (2%) (Fig. 1D).

Pravastatin attenuated carboplatin-induced ROS production, renal cell apoptosis, and caspase-3 expression. Exposure of NRK-52E renal epithelial cells to 100 μM carboplatin for 24 h induced production of ROS approximately 25-fold that in saline-treated cells, as shown by DCF staining (Fig. 2A). This increase in the level of ROS was significantly ($p < 0.05$) attenuated by pretreatment with 50 μM pravastatin for 30 min. Pravastatin also significantly ($p < 0.05$) inhibited carboplatin-induced caspase-3 expression in NRK-52E cells (Fig. 2B). We also performed experiments with cisplatin and showed that this agent induced caspase-3 expression in NRK-52 cells, which was attenuated by treatment with pravastatin (Supplemental Fig. 5).

In vivo experiments showed that i.p. injection of mice with pravastatin significantly (p

Molecular Pharmacology Fast Forward. Published on April 5, 2010 as DOI: 10.1124/mol.109.061101
This article has not been copyedited and formatted. The final version may differ from this version.

< 0.01) reduced not only the rate of apoptosis in kidney cells, from 14% to 3% (Fig. 2C), but also the expression of cleaved, active caspase-3 compared to mice treated with carboplatin alone ($p < 0.05$) (Fig. 2D).

Pravastatin improved renal function and survival in mice treated with carboplatin. Carboplatin treatment resulted in abnormal renal function, as revealed by the levels of serum urea nitrogen and creatinine measured 5 days after injection. This effect was improved by pretreatment with pravastatin (Fig. 3B). In accordance with these markers of renal function, control mice and mice treated with pravastatin showed healthy, histologically comparable tubular systems (Fig. 3Ca, b). However, kidneys of mice treated with carboplatin showed substantial histopathologic changes such as tubular necrosis and dilation, protein casts, and loss of brush borders (Fig. 3Cc). Injection with pravastatin in addition to carboplatin produced marked decreases in these features (Fig. 3Cd).

Survival of mice injected with 100 mg/kg carboplatin was markedly decreased compared to that of control mice. Treatment with pravastatin in addition to carboplatin significantly ($p < 0.01$) increased 7-day survival compared to mice treated with carboplatin alone, as determined by Kaplan-Meier analysis (Fig. 3A).

Pravastatin induction of HO-1 in NRK-52E cells involved cyclooxygenase-2 and a PPARα pathway. To test whether the renal protective effect of pravastatin was mediated by HO-1, NRK-52E cells were treated with 20 μM pravastatin for 24 or 48 h, and the expression

Molecular Pharmacology Fast Forward. Published on April 5, 2010 as DOI: 10.1124/mol.109.061101
This article has not been copyedited and formatted. The final version may differ from this version.

of HO-1 was determined by immunoblotting. As shown in Fig. 4A, the expression of HO-1 was increased after treatment with pravastatin for 24 h. However, HO-1 expression decreased when pravastatin treatment was continued for 48 h.

A similar temporal response was observed when we examined the effect of pravastatin on the expression of cyclooxygenase (COX)-2. To determine whether overexpression of COX-2 might increase the intracellular level of 15d-prostaglandin (PG)I_2, a ligand for PPARα, we examined the effect of 20 μM pravastatin on the level of 6-keto PGF1α (the stable hydrolysis product of PGI_2) with an enzyme immunoassay system. As observed for the expression of COX-2, pravastatin also induced an increase in 6-keto PGF1α at 24 h (Fig. 4B). Similarly, pravastatin increased the levels of PPARα and HO-1 in NRK-52E cells (Fig. 4C).

We next examined whether inhibition of PPARα and COX-2 affected the expression of HO-1. When PPARα was inhibited by transfection of pravastatin-treated cells with plasmid containing PPARα siRNA, the expression of PPARα and HO-1 was reduced (Fig. 4C). When the COX-2 inhibitor NS-398 (Cayman Chemical, Ann Arbor, MI) was added to pravastatin-treated cells, the increase in HO-1 was again significantly decreased, and administration of NS-398 and PPARα siRNA in combination showed a synergistic reduction in the level of HO-1 (Fig. 4D).

Pravastatin enhanced PPARα nuclear translocation in NRK-52E cells. We next examined whether pravastatin enhanced nuclear translocation of PPARα. As shown in Fig.

Molecular Pharmacology Fast Forward. Published on April 5, 2010 as DOI: 10.1124/mol.109.061101
This article has not been copyedited and formatted. The final version may differ from this version.

5A, the level of cytosolic PPARα was not significantly affected by pravastatin in NRK-52E cells transfected with plasmid containing FLAG-PPARα. However, the level of nuclear PPARα was significantly increased in pravastatin-treated cells (Fig. 5A, lane 3 vs lane 4). Immunostaining also showed that FLAG-PPARα translocated from the cytosol to the nucleus in NRK-52E cells treated with pravastatin (Fig. 5Bc). This effect was significantly decreased in cells treated with the COX-2 inhibitor NS-398 (Fig. 5Bd).

Pravastatin-activated *HO-1* gene expression is involved in a PPARα-dependent pathway in NRK-52E cells. To clarify whether the increase in expression of HO-1 induced by pravastatin was dependent on translocation of PPARα, a PPRE primer was designed for electrophoretic mobility shift assay using a PPAR-binding sequence located in the HO-1 promoter (position –621 to –500) from rat DNA. PPARα DNA-binding activity was observed in nuclear extracts of pravastatin-treated NRK-52E cells, and this was markedly suppressed in cells pretreated with unlabeled primer (Fig. 6A). To further examine whether the PPARα protein was located in the nucleus and associated with PPRE, a ChIP assay was performed with control and pravastatin-treated cells. As shown in Fig. 6B, the association of PPARα with the PPRE region of the HO-1 promoter was increased in pravastatin-treated cells.

Finally, to determine the role of pravastatin-induced PPARα in activating PPRE and HO-1 promoter activity, NRK-52E cells were cotransfected with increasing amounts of a luciferase expression vector with the PPRE reporter or a 4.5-kb human HO-1

Molecular Pharmacology Fast Forward. Published on April 5, 2010 as DOI: 10.1124/mol.109.061101
This article has not been copyedited and formatted. The final version may differ from this version.

promoter-reporter construct, along with pcDNA3-retinoid X receptor (RXR) α and pcDNA3-FLAG-PPARα or the PPARα agonist WY14643 (Cayman Chemical). As shown in Fig. 6C, PPARα or RXRα alone slightly increased luciferase activity, but combined transfection with PPARα and RXRα increased luciferase activity by approximately 50-fold in cells with the PPRE reporter and approximately 6-fold in cells with the HO-1 promoter construct. In addition, treatment with pravastatin augmented luciferase activity in both the PPRE and HO-1 promoters compared to cells untreated with pravastatin or transfected with PPARα or RXRα alone. Treatment with WY14643 also increased luciferase activity by approximately 50-fold in cells with the PPRE reporter and approximately 8-fold in cells with the HO-1 promoter. Pravastatin cotreatment further increased luciferase activity in both the PPRE and HO-1 promoters compared to untreated cells.

Pravastatin induced HO-1 expression via a PPARα-dependent pathway in mice. We next subjected C57/B6, H129 wild-type ($PPAR\alpha^{+/+}$), and $PPAR\alpha^{-/-}$ mice to pravastatin injection. After injection of pravastatin for 2 days, expression of PPARα and HO-1 was increased in renal extracts of wild-type C57/B6 (Fig. 7A; mRNA and protein) and wild-type W129 mice (Fig. 7B; protein). However, the increase in HO-1 expression was markedly attenuated in $PPAR\alpha^{-/-}$ mice (Fig. 7B). Another commonly used HMG-CoA reductase inhibitor, simvastatin, had the same effect on HO-1 expression in wild-type and $PPAR\alpha^{-/-}$ mice with or without carboplatin treatment (Supplemental Fig. 6).

Molecular Pharmacology Fast Forward. Published on April 5, 2010 as DOI: 10.1124/mol.109.061101
This article has not been copyedited and formatted. The final version may differ from this version.

Discussion

In a previous study, we showed that carboplatin-induced cardiotoxicity was characterized by marked increases in apoptosis (3- to 5-fold) and in the levels of caspase-3 and ROS in cardiomyocytes and that these effects could be ameliorated by treatment with pravastatin (Cheng et al., 2008). In the present study, we extended this work to include the effects of carboplatin in the kidney. Our findings of increased apoptosis and cleaved caspase-3 in cultured kidney cells and in vivo demonstrated that carboplatin had similar effects to those observed in the cardiac system. In addition, we showed that the levels of ROS also increased in kidney cells exposed to carboplatin, suggesting the involvement of ROS in carboplatin-induced apoptosis. Results of the present study indicate that pretreatment with pravastatin markedly decreased carboplatin-induced renal tissue damage and ameliorated renal dysfunction, consistent with the results of Li, Yang, et al. (2004), who showed that pravastatin normalized serum creatinine levels in a rat model of chronic cyclosporine-induced nephropathy.

The cardioprotective effects of atorvastatin have been shown to involve the upregulation of COX-2 and increased production of PGI_2 (Birnbaum et al., 2005). When we examined the effects of pravastatin on the expression of COX-2 and PGI_2, we found that both were increased in response to pravastatin, suggesting that in kidney cells, pravastatin

Molecular Pharmacology Fast Forward. Published on April 5, 2010 as DOI: 10.1124/mol.109.061101
This article has not been copyedited and formatted. The final version may differ from this version.

stimulates overexpression of COX-2, resulting in increased PGI_2.

PGI_2 is known to mediate the translation of PPARα (Chen et al., 2009). In the present study, we showed that nuclear PPARα was increased in NRK-52E renal epithelial cells in response to treatment with pravastatin and that this increase was the result of translocation of PPARα from the cytoplasm to the nucleus. The observation that translocation was blocked by the addition of the COX-2 inhibitor NS-398 supports the hypothesis that the translocation was mediated by PGI_2.

Many lines of inquiry have pointed to a prominent cytoprotective role for HO-1 in modulating tissue responses to injury (reviewed by Sikorski et al., 2004). In a rat model of renal ischemia-reperfusion injury, Gueler et al. (2007) showed that pretreatment with cervistatin decreased renal damage and dysfunction after ischemia-reperfusion. These authors found that HO-1 expression was increased after ischemia-reperfusion, that the increased expression was significantly greater in rats pretreated with cervistatin, and that the protective effect of statin was completely abolished by cotreatment with a competitive inhibitor of HO-1. Grosser et al. (2004) reported that treatment of endothelial cells with statins resulted in activation of the HO-1 promoter, along with accumulation of HO-1 transcript and protein. In a study of vascular smooth muscles cells, Lee et al. (2004) reported that simvastatin increased the level of HO-1 and suggested that p38 and the phosphatidylinositol-3-kinase and protein kinase B (PI3K-Akt) pathway might be involved. Our present findings of significantly

Molecular Pharmacology Fast Forward. Published on April 5, 2010 as DOI: 10.1124/mol.109.061101
This article has not been copyedited and formatted. The final version may differ from this version.

increased levels of HO-1 transcript and protein in the kidneys of pravastatin-pretreated mice after carboplatin-induced renal injury are consistent with these previous findings in rats. In addition, we demonstrated that this effect was mediated by PGI_2 and PPARα. This was further corroborated by our in vitro data, in which we showed that pravastatin treatment increased expression of PGI_2, PPARα, and HO-1 in cultured renal tubule cells.

The work of Krönke et al. (2007) in human vascular cells showed that the HO-1 promoter contains a PPRE and that HO-1 is transcriptionally regulated by PPARα. We showed PPRE-binding activity in nuclear extracts of pravastatin-treated NRK-52E cells, that PPARα was associated with the HO-1 promoter, and that the association was stimulated by pravastatin. Finally we showed that PPARα and RXRα increased expression of a plasmid construct containing the HO-1 promoter and that this expression was stimulated by pravastatin.

Our in vitro results showing inhibition of pravastatin-induced HO-1 activation by NS-398 and PPARα siRNA further support the hypothesis that, in kidney cells, activation of HO-1 by pravastatin involves in a PPARα-dependent pathway. Our experiments in PPARα-knockout mice confirmed that in vivo, as in vitro, the increase in HO-1 expression stimulated by treatment with pravastatin was, to some extent, dependent on a PPARα pathway.

Taken together, our data support a relation between pravastatin and HO-1. Pravastatin

Molecular Pharmacology Fast Forward. Published on April 5, 2010 as DOI: 10.1124/mol.109.061101
This article has not been copyedited and formatted. The final version may differ from this version.

induces overexpression of COX-2, which upregulates PGI_2. PGI_2 then promotes the translocation of PPARα to the nucleus, where it binds PPRE and induces the expression of HO-1.

Because HO-1 plays a cytoprotective role in modulating the responses of many tissues to different types of injury and pathologic states, it is not surprising that there would be numerous complex tissue-specific inducers that lead to its increased expression. The cardioprotective effects of atorvastatin have been shown to be mediated by the increased production of multiple prostaglandins, including cytosolic phospholipase A_2 ($cPLA_2$), PGI_2, and PGE_2, via upregulation of COX-2 (Birnbaum et al., 2005). Whether prostaglandins other than PGI_2, such as PGE_2 and PGJ_2, augment PPARα translocation and activate HO-1 expression in our carboplatin-induced renal injury model will require further study. In addition, PPARs other than PPARα can be activated by statins. For example, Yano et al. (2007) reported that statins activate PPARγ in macrophages. We have not ruled out a role for PPARγ in our model.

HO-1 degrades heme into CO and biliverdin, which have powerful anti-inflammatory, antiapoptotic, and antioxidant effects. This likely accounts for the beneficial effect of pravastatin in inhibiting carboplatin-induced nephrotoxicity. However, these heme degradation products are also potentially injurious. Indeed, simvastatin induction of HO-1 has been shown to be mediated by nuclear factor erythroid 2-related factor 2 (Nrf2) in Neuro 2A

Molecular Pharmacology Fast Forward. Published on April 5, 2010 as DOI: 10.1124/mol.109.061101
This article has not been copyedited and formatted. The final version may differ from this version.

cells, and its upregulation was significantly associated with increased apoptosis in that system (Hsieh et al., 2008). The multiple pathways for induction of HO-1 may work synergistically to optimize its expression under many different circumstances. Thus, the pathway we have proposed is likely to be one of several, if not many, that regulates the expression of HO-1 and one of several that mediates the pleiotropic effects of statins.

Our present data showed that carboplatin at a single high dose (100 mg/kg) induced renal dysfunction in mice, as evidenced by elevated levels of blood urea nitrogen and creatinine. It is important to note that these parameters of nephrotoxicity were observed at least 5 days after administration of carboplatin; whereas the survival of mice continued to decline until day 7. The decrease in survival produced by carboplatin in mice may be the result of both nephrotoxicity and cardiomyopathy (Cheng et al., 2008). In addition, impaired renal activity and suppressed renal expression of antioxidant enzymes may be involved (Husain et al., 2004). Our present results showed that lower doses of carboplatin (50 mg/kg) did not alter the level of blood urea nitrogen or creatinine (data not shown) or 7-day survival in mice. Therefore, both dose and time of carboplatin exposure are probably important in causing nephrotoxicity.

An interesting observation from the present study is that pravastatin did not completely protect mice against carboplatin-induced nephrotoxicity (Figs. 2 and 3). Similar partial effects of other statins, including cervistatin and atorvastatin, on renal ischemia-reperfusion

injury have been reported (Gueler et al., 2007; Gottman et al., 2007). Although the exact reason for the insufficient effect of pravastatin is not clear at present, one possible explanation involves an inhibitory activity of pravastatin on the mammalian target of rapamycin (mTOR) pathway (Roudier et al., 2006). Therefore, increases in the mTOR response as a consequence of pravastatin treatment may partially mask pravastatin's beneficial effect on carboplatin-induced kidney injury. Additional studies of mTOR activity are needed to further explore whether these mechanisms are important for the antiapoptotic effect mediated by pravastatin in vitro and in vivo.

In the present study, we administered pravastatin to mice at a dose of 1 mg/kg. This dose was lower than the daily therapeutic dose in humans (20–80 mg/kg/day) (McLean et al., 2008). However, when we increased the dose to 10 mg/kg in mice subjected to carboplatin treatment, the survival rate was significantly decreased compared to that in mice receiving doses of 5 mg/kg or 1 mg/kg (data not shown). This result is in conflict with that of a previous study that used pravastatin (100–150 mg/kg) to inhibit ischemia-reperfusion–induced nephrotoxicity (Sharyo et al., 2008). It is possible that the high dose of carboplatin used in our present study augmented the expression of inducible nitric oxide synthase (Ikeda et al., 2001) and contributed to the greater production of oxidative stress compared to that in the ischemia-reperfusion model. On the basis of our results, we conclude that low doses of pravastatin have the potential to provide effective protection

Molecular Pharmacology Fast Forward. Published on April 5, 2010 as DOI: 10.1124/mol.109.061101
This article has not been copyedited and formatted. The final version may differ from this version.

against nephrotoxicity induced by carboplatin. However, higher doses must be administrated carefully. Further clinical evaluations in humans are needed to determine whether pravastatin would be an attractive drug for the treatment of acute renal injury.

In summary, this study presents a novel mechanism underlying the antiapoptotic action of pravastatin, which confers protection against carboplatin-induced injury in the kidney. In addition, our data highlight the critical role of PGI_2-mediated PPARα translocation in the induction of *HO-1* gene expression. Thus, overexpression of PPARα, either by treatment with pravastatin or gene delivery, may offer a viable strategy to prevent acute renal cell damage and improve the outcome of carboplatin-induced injury in the kidney.

References

Agarwal A, Balla J, Alam J, Croatt AJ, Nath KA (1995) Induction of heme oxygenase in toxic renal injury: a protective role in cisplatin nephrotoxicity in the rat. *Kidney Int* **48**: 1298-1307.

Alberts DS (1995) Carboplatin versus cisplatin in ovarian cancer. *Semin Oncol* **22**: 88-90.

Birnbaum Y, Ye Y, Rosanio S, Tavackoli S, Hu ZY, Schwarz ER, Uretsky BF (2005) Prostaglandins mediate the cardioprotective effects of atorvastatin against ischemia-reperfusion injury. *Cardiovas Res* **65**: 345-355.

Chen HH, Chen TW, Lin H (2009) Prostacyclin-induced peroxisome proliferator-activated receptor α translocation attenuates NF-κB and TNF-α activation after renal ischemia-reperfusion injury. *Am J Physiol Renal Physiol* **July 29**: Epub ahead of print.

Cheng CF, Juan SH, Chen JJ, Chao YC, Chen HH, Lian WS, Lu CY, Chang CI, Chiu TH, Lin H (2008) Pravastatin attenuates carboplatin-induced cardiotoxicity via inhibition of oxidative stress associated apoptosis. *Apoptosis* **13**: 883-894.

Cuturi MC, Christoph F, Woo J, Iyer S, Brouard S, Heslan JM, Pignon P, Soulillou JP, Buelow R (1999) RDP1258, a new rationally designed immunosuppressive peptide, prolongs allograft survival in rats: analysis of its mechanism of action. *Mol Med* **5**: 820-832.

Ferrándiz ML, Devesa I (2008) Inducers of heme oxygenase-1. *Curr Pharm Des* **14**: 473-486.

Forman BM, Chen J, Evans RM (1997) Hypolipidemic drugs, polyunsaturated fatty acids, and eicosanoids are ligands for peroxisome proliferator-activated receptors α and δ. *Proc Nat Acad Sci U S A* **94**: 4312-4317.

Fujiwara K, Sakuragi N, Suzuki S, Yoshida N, Maehata K, Nishiya M, Koshida T, Sawai H, Aotani E, Kohno I (2003) First-line intraperitoneal carboplatin-based chemotherapy for 165 patients with epithelial ovarian carcinoma: results of long-term follow-up. *Gynecol Oncol* **90**: 637-643.

Gottmann U, Brinkkoetter PT, Hoeger S, Gutermann K, Coutinho ZM, Ruf T, Hui S, Liu Z, Schnuelle P, van der Woude FJ, Braun C, Yard BA (2007) Atorvastatin donor pretreatment prevents ischemia/reperfusion injury in renal transplantation in rats: possible role for aldose-reductase inhibition. *Transplantation* **84**: 755-762.

Grosser N, Hemmerle A, Berndt G, Erdmann K, Hinkelmann U, Schürger S, Wijayanti N, Immenschuh S, Schröder H (2004) The antioxidant defense protein heme oxygenase 1 is a novel target for statins in endothelial cells. *Free Radic Biol Med* **37**: 2064-2071.

Gueler F, Park JK, Rong S, Kirsch T, Lindschau C, Zheng W, Elger M, Fiebeler A, Fliser D, Luft FC, Haller H (2007) Statins attenuate ischemia-reperfusion injury by inducing heme oxygenase-1 in infiltrating macrophages. *Am J Pathol* **170**: 1192-1199.

Gueler F, Rong S, Park JK, Fiebeler A, Menne J, Elger M, Mueller DN, Hampich F, Dechend R, Kunter U, Luft FC, Haller H (2002) Postischemic acute renal failure is reduced by

short-term statin treatment in a rat model. *J Am Soc Nephrol* **13**: 2288-2298.

Hsieh CH, Rau CS, Hsieh MW, Chen YC, Jeng SF, Lu TH, Chen SS (2008) Simvastatin-induced heme oxygenase-1 increases apoptosis of Neuro 2A cells in response to glucose deprivation. *Toxicol Sci* **101**: 112-121.

Husain K, Whitworth C, Rybak LP (2004) Time response of carboplatin-induced nephrotoxicity in rats. *Pharmacol Res* **50**: 291-300.

Ikeda U, Shimpo M, Ikeda M, Minota S, Shimada K (2001) Lipophilic statins augment inducible nitric oxide synthase expression in cytokine-stimulated cardiac myocytes. *J Cardiovasc Pharmacol* **38**: 69-77.

Kintzel PE (2001) Anticancer drug-induced kidney disorders. *Drug Saf* **24**: 19-38.

Krönke G, Kadl A, Ikonomu E, Blüml S, Fürnkranz A, Sarembock IJ, Bochkov VN, Exner M, Binder BR, Leitinger N (2007) Expression of heme oxygenase-1 in human vascular cells is regulated by peroxisome proliferator-activated receptors. *Ateriosclerosis Thromb Vasc Biol* **27**: 1276-1282.

Lee TS, Chang CC, Zhu Y, Shyy JY (2004) Simvastatin induces heme oxygenase-1: a novel mechanism of vessel protection. *Circulation* **110**: 1296-1302.

Li S, Wu P, Yarlagadda P, Vadjunec NM, Proia AD, Harris RA, Portilla D (2004) PPARα ligand protects during cisplatin-induced acute renal failure by preventing inhibition of renal FAO and PDC activity. *Am J Physiol Renal Physiol* **286**: F572-F580.

Li C, Yang CW, Park JH, Lim SW, Sun BK, Jung JY, Kim SB, Kim YS, Kim J, Bang BK (2004) Pravastatin treatment attenuates interstitial inflammation and fibrosis in a rat model of chronic cyclosporine-induced nephrophathy. *Am J Physiol Renal Physiol* **286**: F46-F57.

Lin H, Cheng CF, Hou HH, Lian WS, Chao YC, Ciou YY, Djoko B, Tsai MT, Cheng CJ, Yang RB (2008) Disruption of guanylyl cyclase-G protects against acute renal injury. *J Am Soc Nephrol* **19**: 339-348.

McLean DS, Ravid S, Blazing M, Gersh B, Shui A, Cannon CP (2008) Effect of statin dose on incidence of atrial fibrillation: data from the Pravastatin or Atorvastatin Evaluation and Infection Therapy-Thrombolysis in Myocardial Infarction 22 (PROVE IT-TIMI 22) and Aggrastat to Zocor (A to Z) trials. *Am Heart J* **155**: 298-302.

Nath KA, Grande JP, Haggard JJ, Croatt AJ, Katusic ZS, Solovey A, Hebbel RP (2001) Oxidative stress and induction of heme oxygenase-1 in the kidney in sickle cell disease. *Am J Pathol* **158**: 893-903.

Pivot X, Cals L, Cupissol D, Guardiola E, Tchiknavorian X, Guerrier P, Merad L, Wendling JL, Barnouin L, Savary J, Thyss A, Schneider M (2001) Phase II trial of a paclitaxel-carboplatin combination in recurrent squamous cell carcinoma of the head and neck. *Oncology* **60**: 66-71.

Roudier E, Mistafa O, Stenius U (2006) Statins induce mammalian target of rapamycin

(mTOR)-mediated inhibition of Akt signaling and sensitize p53-deficient cells to cytostatic drugs. *Mol Cancer Ther* **5**: 2706-2715.

Sharyo S, Yokota-Ikeda N, Mori M, Kumagai K, Uchida K, Ito K, Burne-Taney MJ, Rabb H, Ikeda M (2008) Provastatin improves renal ischemia-reperfusion injury by inhibiting the mevalonate pathway. *Kidney Int* **74**: 577-584.

Sikorski EM, Hock T, Hill-Kapturczak N, Agarwal A (2004) The story so far: Molecular regulation of the heme oxygenase-1 gene in renal injury. *Am J Physiol Renal Physiol* **286**: F425-F441.

Takemoto M, Liao JK (2001) Pleiotropic effects of 3-hydroxy-3-methylglutaryl coenzyme a reductase inhibitors. *Arterioscler Thromb Vas Biol* **21**: 1712-1719.

Yano M, Matsumura T, Senokuchi T, Ishii N, Murata Y, Taketa K, Motoshima H, Taguchi T, Sonoda K, Kukidome D, Takuwa Y, Kawada T, Brownlee M, Nishikawa T, Araki E (2007) Statins activate peroxisome proliferator-activated receptor γ through extracellular signal-regulated kinase 1/2 and p38 mitogen-activated protein kinase-dependent cyclooxygenase-2 expression in macrophages. *Circ Res* **100**: 1442-1451.

Molecular Pharmacology Fast Forward. Published on April 5, 2010 as DOI: 10.1124/mol.109.061101
This article has not been copyedited and formatted. The final version may differ from this version.

Figure Legends

Fig. 1. Carboplatin-induced expression of caspase-3 and apoptosis in kidney cells in vitro and in vivo. (A, B) Concentration- and time-dependent expression of caspase-3 in NRK-52E renal epithelial cells. NRK-52E cells were treated with carboplatin (50–800 μM) for 0 to 48 h, and caspase-3 expression was analyzed by immunoblotting. (C) Evaluation of caspase-3 expression in mice after treatment with carboplatin. C57/B6 mice were injected with 100 mg/kg carboplatin intraperitoneally, and cytosolic fractions of homogenized kidney were prepared at the indicated time points (1–2 days) and immunoblotted with antibody against caspase-3. (D) Carboplatin-induced apoptosis in mouse kidney. Mice were injected with 100 mg/kg carboplatin intraperitoneally for 2 days, and paraformaldehyde-fixed sections were prepared and stained with the terminal deoxynucleotidyl transferase dUTP nick end labeling (TUNEL) method. Histograms represent the numbers of TUNEL-positive cells (quantitative analysis of TUNEL-positive nuclei relative to total nuclei) in carboplatin-treated (100 mg/kg) (a) and control (b) mice from three independent experiments. Bar = 200 μm. $^{**}p < 0.01$.

Fig. 2. Pravastatin-inhibited production of reactive oxygen species (ROS), caspase-3 expression, and apoptosis in response to carboplatin treatment. (A) Levels of ROS after treatment with carboplatin or pravastatin in vitro. NRK-52E cells were subjected to 100 μM carboplatin for 24 h with no additional treatment (c) or with a 30-min pre-exposure to 50 μM

Molecular Pharmacology Fast Forward. Published on April 5, 2010 as DOI: 10.1124/mol.109.061101
This article has not been copyedited and formatted. The final version may differ from this version.

pravastatin (d). Cells shown in (a) and (b) were subjected to saline and pravastatin treatment alone, respectively. The intracellular ROS concentration was determined according to dichlorodihydrofluorescein (DCF) fluorescence, as described in the Materials and Methods. *$p < 0.05$ compared to carboplatin treatment. (B) Protein level of caspase-3 in NRK-52E cells. *$p < 0.05$ compared to carboplatin treatment. (C) Terminal deoxynucleotidyl transferase dUTP nick end labeling (TUNEL) staining of kidney sections from carboplatin-treated mice (a) and pravastatin-treated mice (b). Histograms represent numbers of TUNEL-positive cells in carboplatin-treated mice with or without pretreatment with pravastatin (n = 5 animals in each group). Representative results of three separate experiments are shown. Bar = 200 μm. **$p < 0.01$. (D) Expression of active caspase-3 protein in mice. Renal lysates from each mouse were treated as indicated and probed with specific antibody against the cleaved, active form of caspase-3. Data represent results from three independent experiments. Scanning densitometry was used for semiquantitative analysis compared to β-actin. *$p < 0.05$ compared to carboplatin treatment.

Fig. 3. Pravastatin decreased carboplatin-induced renal dysfunction and improved survival in mice. (A) Cumulative survival after pravastatin treatment in carboplatin-injected mice. Mice were injected intraperitoneally with pravastatin for 1 day before carboplatin treatment (100 mg/kg). Kaplan-Meier survival curves showed better survival in the pravastatin + carboplatin

group (~60%) compared to carboplatin treatment alone (~20%) over a 7-day period. (B) Effect of pravastatin on renal function in mice after carboplatin treatment. Mice were injected with pravastatin for 1 day and injected intraperitoneally with carboplatin (100 mg/kg) 2 days later. Serum urea nitrogen and creatinine levels were measured 5 days after administration of carboplatin. $^{**}p < 0.01$ compared to carboplatin treatment. (C) Photomicrographs of kidneys from carboplatin-treated mice (c) show severe renal failure, including extensive loss of brush borders (blue arrow) and tubular necrosis (black arrow). Injection with pravastatin produced a marked decrease in the severity of these features (d). (a and b) control mice and mice treated with pravastatin alone, respectively. Sections were stained with hematoxylin and eosin. Bar = 200 μm.

Fig. 4. Effect of pravastatin on heme oxygenase (HO)-1 expression via a peroxisome proliferator-activated receptor (PPAR) α–dependent pathway. (A) Pravastatin induced expression of HO-1 and cyclooxygenase (COX)-2 in a time-dependent manner. Rat NRK-52E renal epithelial cells were treated with 20 μM pravastatin for 24 or 48 h, and HO-1 and COX-2 levels were analyzed by immunoblotting. Representative results of three independent experiments are shown. (B) Supernatants were assayed for PGI_2 concentration by 6-keto prostaglandin (PG) F1α enzyme-linked immunosorbent assay. $^{**}p < 0.01$ compared to pravastatin treatment. (C) Protein levels of PPARα and HO-1 in

Molecular Pharmacology Fast Forward. Published on April 5, 2010 as DOI: 10.1124/mol.109.061101
This article has not been copyedited and formatted. The final version may differ from this version.

pravastatin-treated cells after transfection with a plasmid encoding PPARα siRNA. *$p < 0.05$ and **$p < 0.01$ compared to pravastatin treatment. (D) Protein level of HO-1 in pravastatin-treated cells after pretreatment with the COX-2 inhibitor NS-398 for 30 min. Cell lysates were blotted with antibody against HO-1. Representative results from three independent experiments are shown. Scanning densitometry was used for semiquantitative analysis to compare against β-actin. *$p < 0.05$, **$p < 0.01$.

Fig. 5. Enhanced nuclear translocation of peroxisome proliferator-activated receptor (PPAR) α in response to pravastatin via a PPARα-PGI_2–dependent pathway. (A) Translocation of PPARα in response to pravastatin treatment. Plasmid containing FLAG-PPARα was transfected into NRK-52E cells, and cell lysates were separated into nuclear and cytosolic fractions and probed with specific antibody against FLAG. Representative results from two independent experiments are shown. Scanning densitometry was used for semiquantitative analysis to compare against β-actin. *$p < 0.05$ compared to sham treatment. (B) Subcellular localization of FLAG-PPARα in pravastatin-treated NRK-52E cells. (a and b) In control cells without pravastatin treatment, most of the FLAG-PPARα was located in the cytosol. (c) After pravastatin treatment, PPARα was translocated from the cytosol to the nucleus. (d) Nuclear translocation was decreased by pretreatment with the cyclooxygenase (COX)-2 inhibitor NS-398. Bar = 200 μm.

Molecular Pharmacology Fast Forward. Published on April 5, 2010 as DOI: 10.1124/mol.109.061101
This article has not been copyedited and formatted. The final version may differ from this version.

Fig. 6. Pravastatin enhanced expression of heme oxygenase (HO)-1 by a peroxisome proliferator-activated receptor (PPAR) α-PGI_2–dependent pathway. (A) Binding activity of PPARα in the peroxisome proliferator response element (PPRE)-binding site of the HO-1 promoter. Results of electrophoretic mobility shift assay with the PPARα probe in nuclear extracts of NRK-52E cells with or without treatment with pravastatin and in the presence of 0, 10×, or 100× concentration of unlabeled competitor probe. P = probe alone; C = cells alone. (B) Chromatin was isolated from pravastatin-treated or untreated NRK-52E cells after transfection with FLAG-PPARα plasmid. Chromatin immunoprecipitation (ChIP) experiments were carried out with FLAG-specific antibody and primers to amplify –621 to –500 of the HO-1 locus, which contains one predicted PPAR-binding site in rats. Immunoprecipitated DNA was quantified by quantitative polymerase chain reaction with a TaqMan-labeled probe and normalized to the quantity of DNA in 10% of the input used for ChIP for each sample. The data are representative of two to four independent experiments. (C) Pravastatin induced PPRE and HO-1 promoter activity in a PPARα-dependent manner. NRK-52E cells were transiently cotransfected with reporter construct pGL2-PPRE or pGL2 containing the HO-1-α promoter, pcDNA3.1-RXRα, or FLAG-PPARα 2 days after treatment with or without pravastatin and/or the PPARα agonist WY14643 (200 μM) for 24 h. The pGL2-basic plasmid served as a vector control. Cells were collected and assayed for

Molecular Pharmacology Fast Forward. Published on April 5, 2010 as DOI: 10.1124/mol.109.061101
This article has not been copyedited and formatted. The final version may differ from this version.

luciferase activity. *$p < 0.05$.

Fig. 7. Effect of pravastatin on heme oxygenase (HO)-1 expression in wild-type (peroxisome proliferator-activated receptor [PPAR] $\alpha^{+/+}$) and PPAR$\alpha^{-/-}$ mice. (A) mRNA (*top*) and protein (*bottom*) expression of PPARα and HO-1 after intraperitoneal injection of pravastatin in mice. *$p < 0.05$ compared to sham treatment. (B) Expression of HO-1 protein in wild-type (n = 5 in each group) and PPAR$\alpha^{-/-}$ mice (n = 7 in each group) with or without pravastatin treatment.

Fig.1

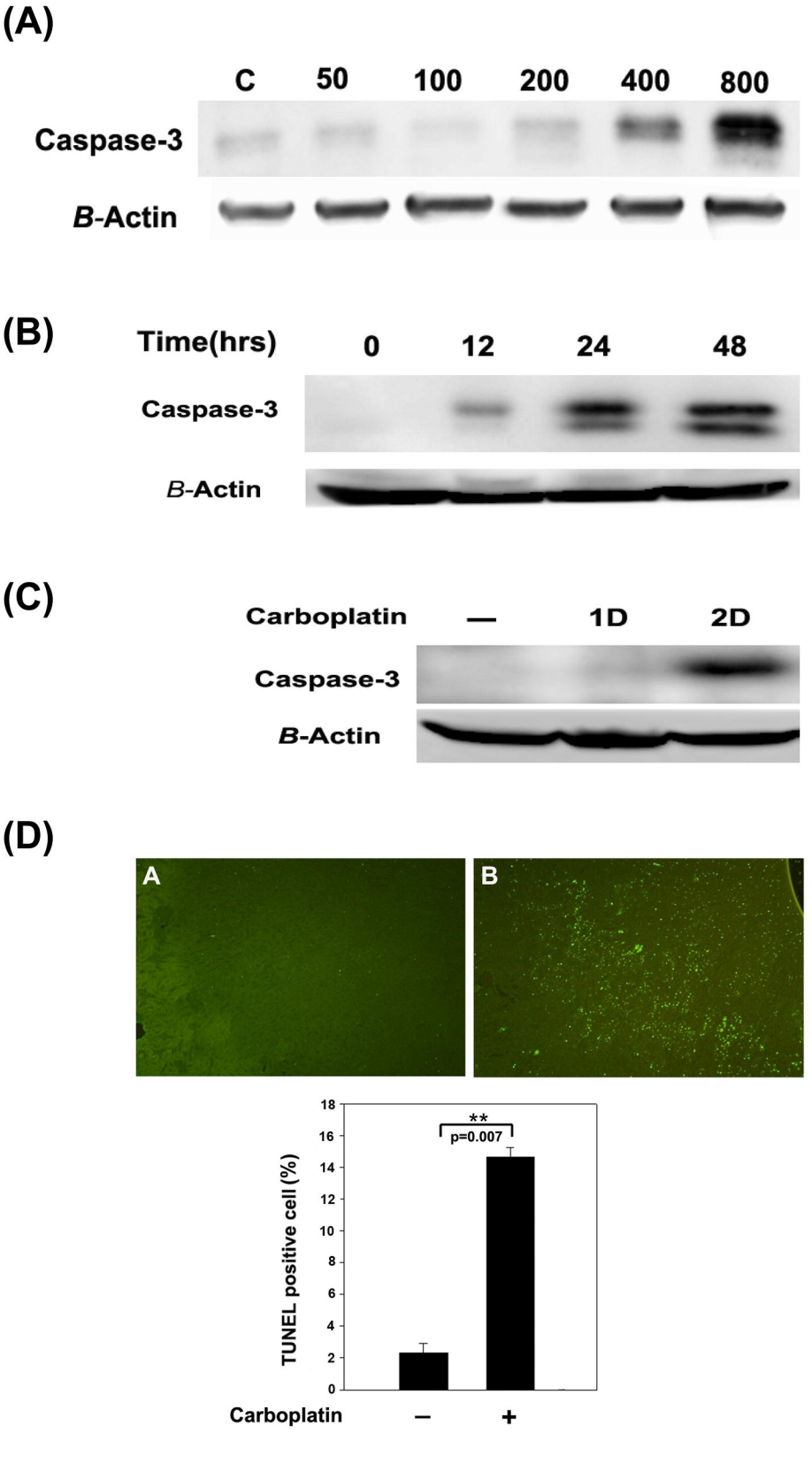
(A)
C
50
100
200
400
800
Caspase-3
B-Actin
(B)
Time(hrs)
0
12
24
48
Caspase-3
B-Actin
(C)
Carboplatin
—
1D
2D
Caspase-3
B-Actin
(D)
A
B
TUNEL positive cell (%)
18
16
14
12
10
8
6
4
2
0
**
p=0.007
Carboplatin
–
+

Fig.2

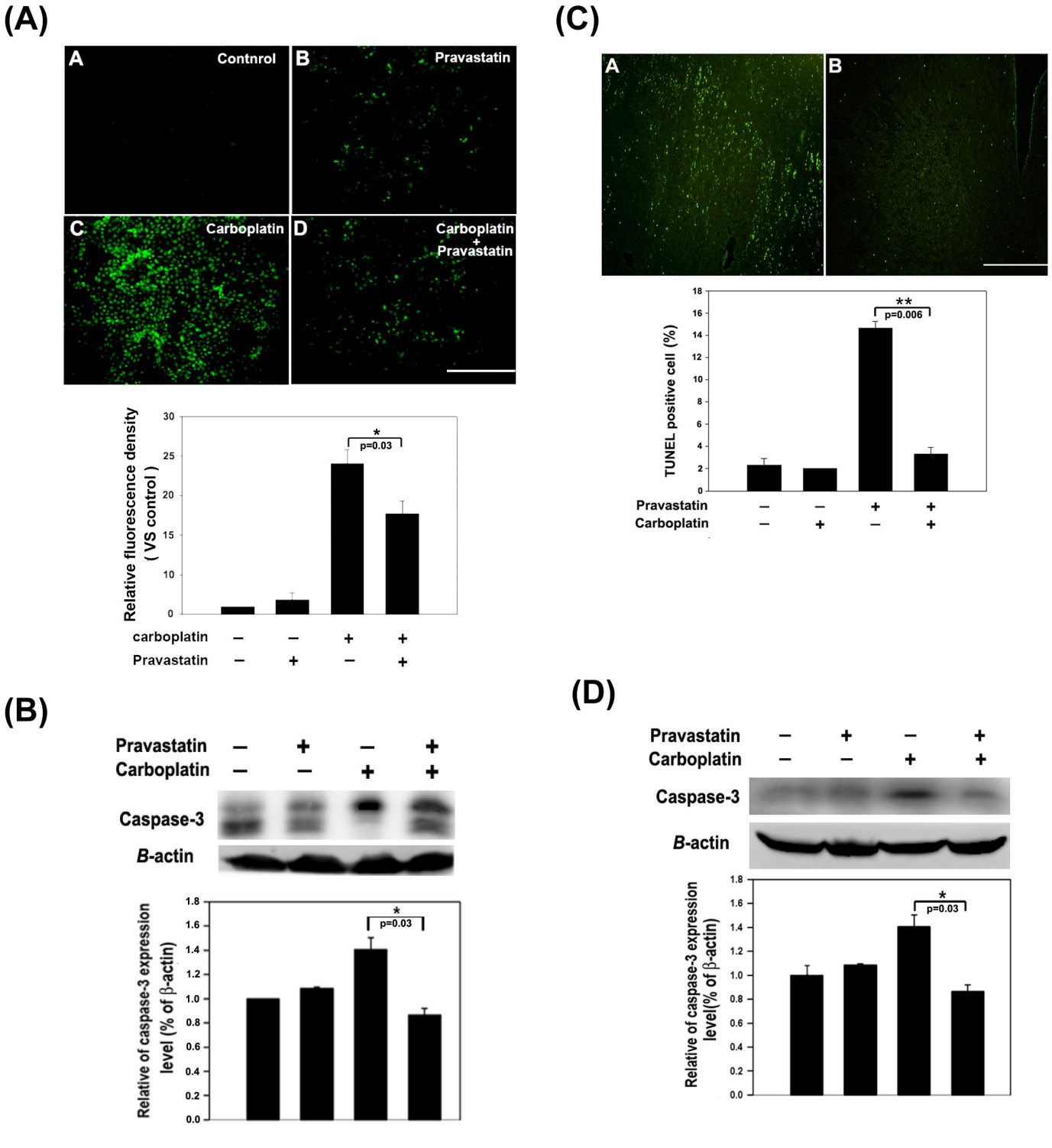
(A)
A
Contnrol
B
Pravastatin
C
Carboplatin
D
Carboplatin + Pravastatin
Relative fluorescence density (VS control)
*
p=0.03
carboplatin
Pravastatin
(C)
A
B
TUNEL positive cell (%)
**
p=0.006
Pravastatin
Carboplatin
(B)
Pravastatin
Carboplatin
Caspase-3
B-actin
Relative of caspase-3 expression level (% of β-actin)
*
p=0.03
(D)
Pravastatin
Carboplatin
Caspase-3
B-actin
Relative of caspase-3 expression level(% of β-actin)
*
p=0.03

Fig.3

(A)

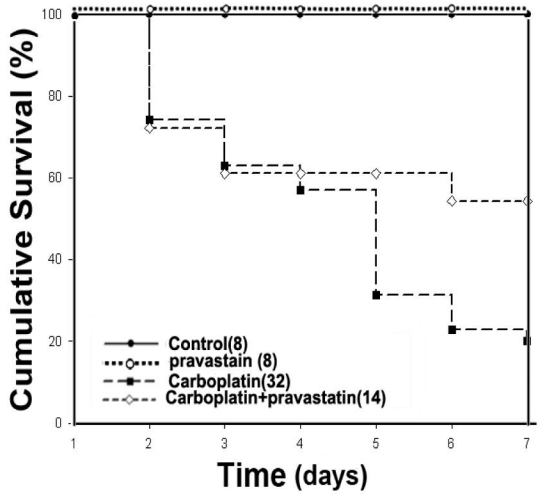
Cumulative Survival (%)
100
80
60
40
20
0
1
2
3
4
5
6
7
Time (days)
Control(8)
pravastain (8)
Carboplatin(32)
Carboplatin+pravastatin(14)

(B)

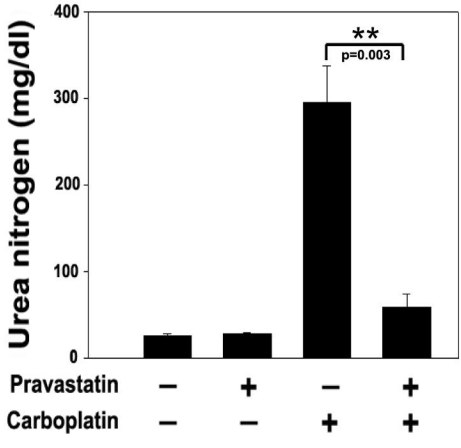
Urea nitrogen (mg/dl)
400
300
200
100
0
**
p=0.003
Pravastatin – + – +
Carboplatin – – + +

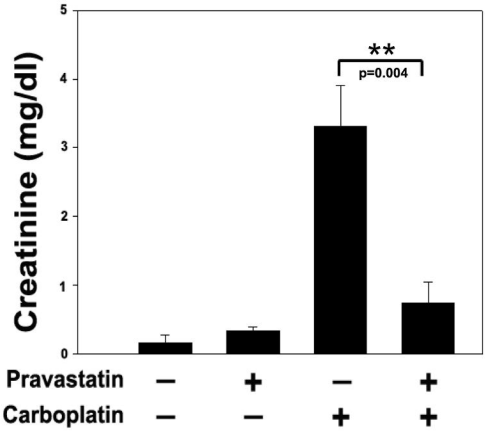
Creatinine (mg/dl)
5
4
3
2
1
0
**
p=0.004
Pravastatin – + – +
Carboplatin – – + +

(C)

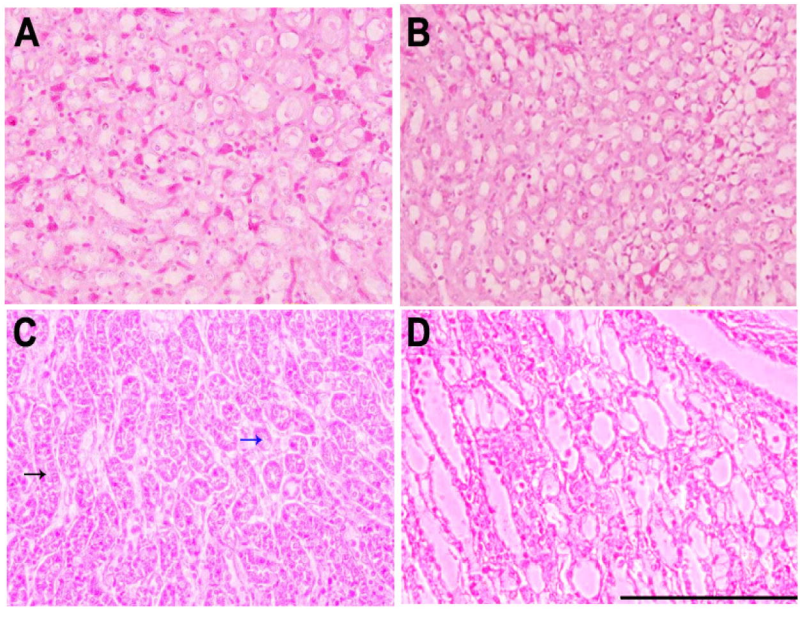
A
B
C
D

Fig.4

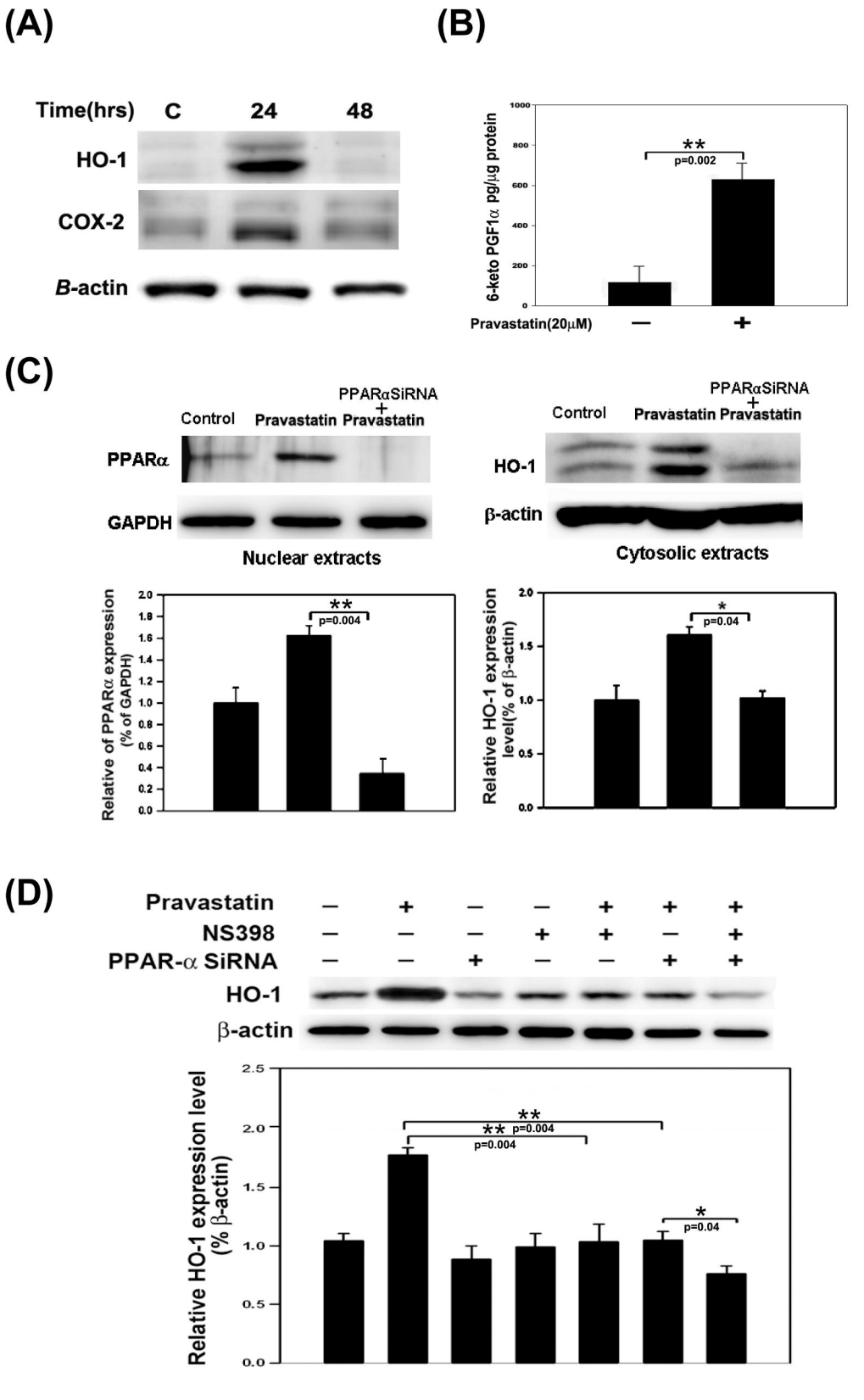
(A)
Time(hrs) C 24 48
HO-1
COX-2
B-actin
(B)
6-keto PGF1α pg/μg protein
**
p=0.002
Pravastatin(20μM) — +
(C)
Control
Pravastatin
PPARαSiRNA + Pravastatin
PPARα
GAPDH
Nuclear extracts
HO-1
β-actin
Cytosolic extracts
Relative of PPARα expression (% of GAPDH)
**
p=0.004
Relative HO-1 expression level(% of β-actin)
*
p=0.04
(D)
Pravastatin
NS398
PPAR-α SiRNA
HO-1
β-actin
Relative HO-1 expression level (% β-actin)
**
** p=0.004
p=0.004
*
p=0.04

Fig.5

(A)

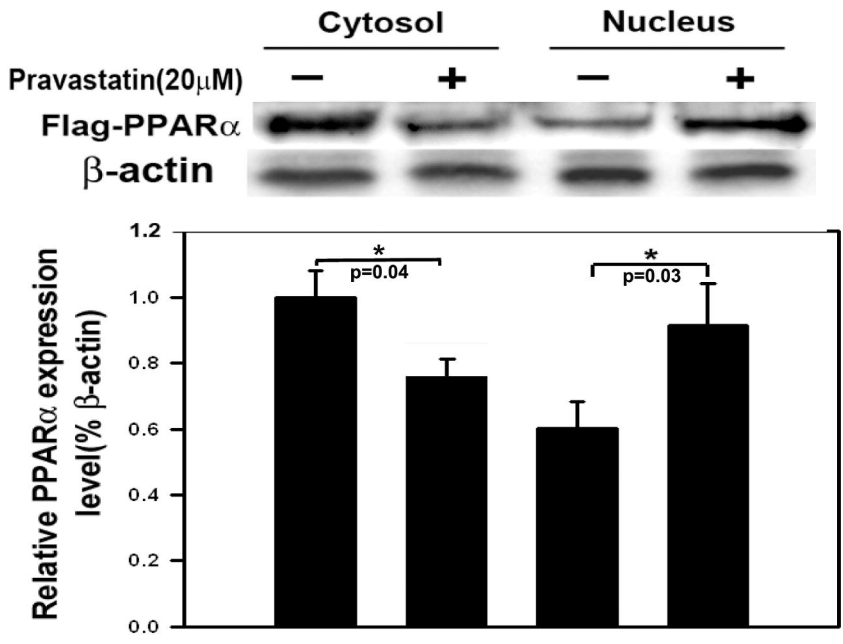
Cytosol
Nucleus
Pravastatin(20μM)
−
+
−
+
Flag-PPARα
β-actin
Relative PPARα expression level(% β-actin)
1.2
1.0
0.8
0.6
0.4
0.2
0.0
*
p=0.04
*
p=0.03

(B)

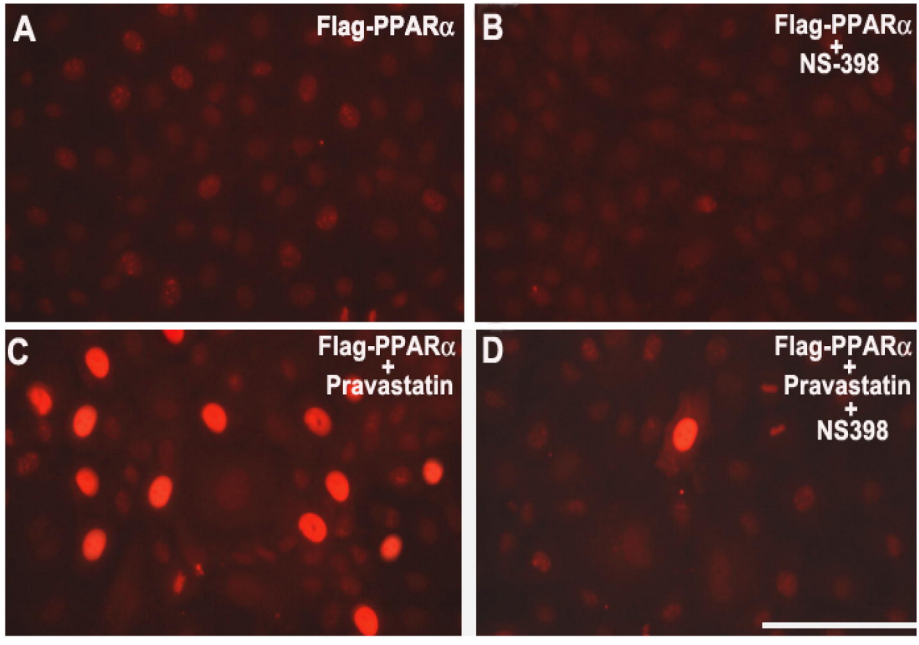
A
Flag-PPARα
B
Flag-PPARα
+
NS-398
C
Flag-PPARα
+
Pravastatin
D
Flag-PPARα
+
Pravastatin
+
NS398

Fig.6

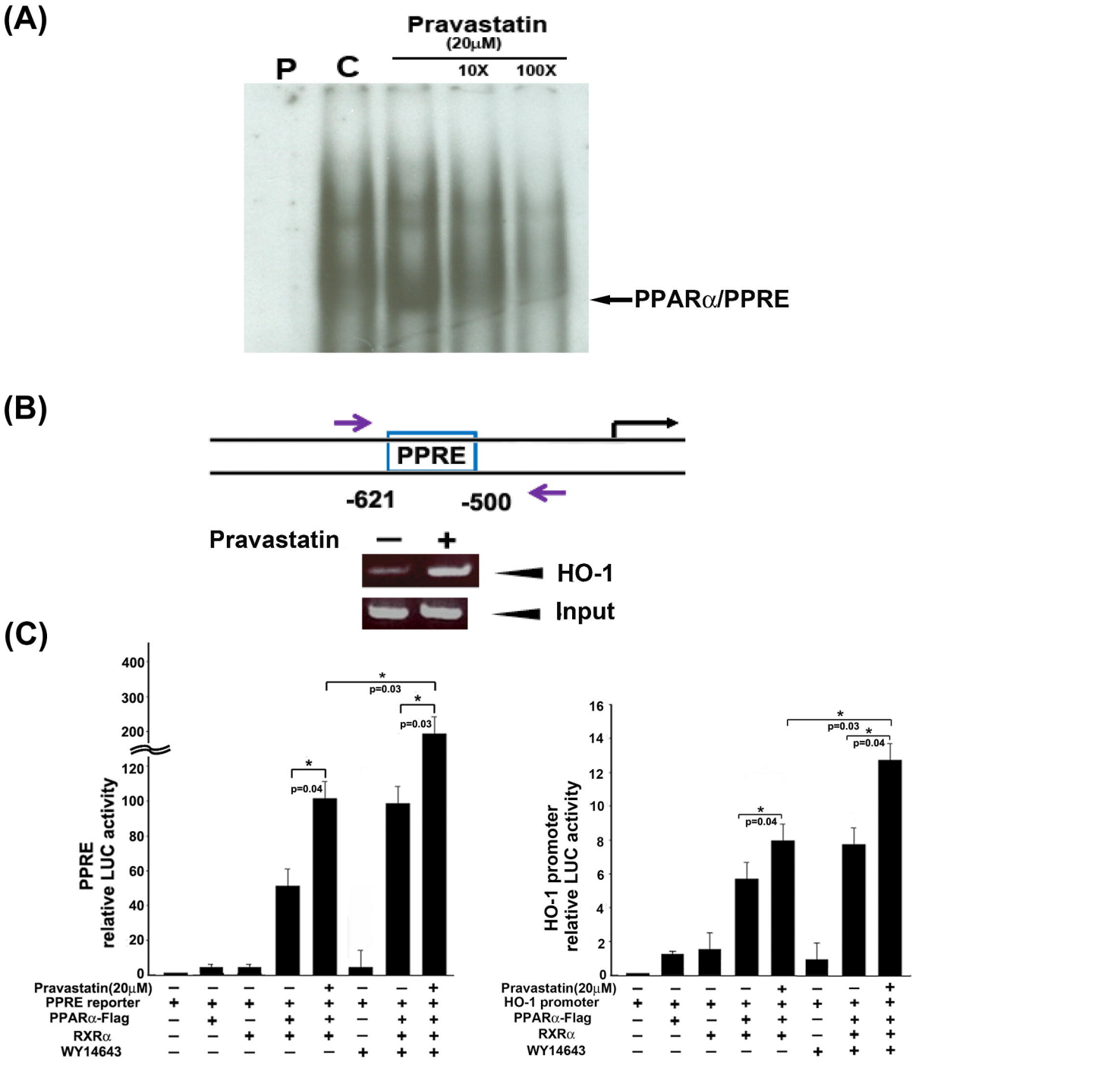
(A)
Pravastatin
(20μM)
P
C
10X
100X
PPARα/PPRE
(B)
PPRE
-621
-500
Pravastatin
—
+
HO-1
Input
(C)
PPRE
relative LUC activity
400
300
200
120
100
80
60
40
20
0
*
p=0.03
*
p=0.03
*
p=0.04
Pravastatin(20μM) — — — — + — — +
PPRE reporter + + + + + + + +
PPARα-Flag — + — + + — + +
RXRα — — + + + — + +
WY14643 — — — — — + + +
HO-1 promoter
relative LUC activity
16
14
12
10
8
6
4
2
0
*
p=0.03
*
p=0.04
*
p=0.04
Pravastatin(20μM) — — — — + — — +
HO-1 promoter + + + + + + + +
PPARα-Flag — + — + + — + +
RXRα — — + + + — + +
WY14643 — — — — — + + +

Fig.7

(A)

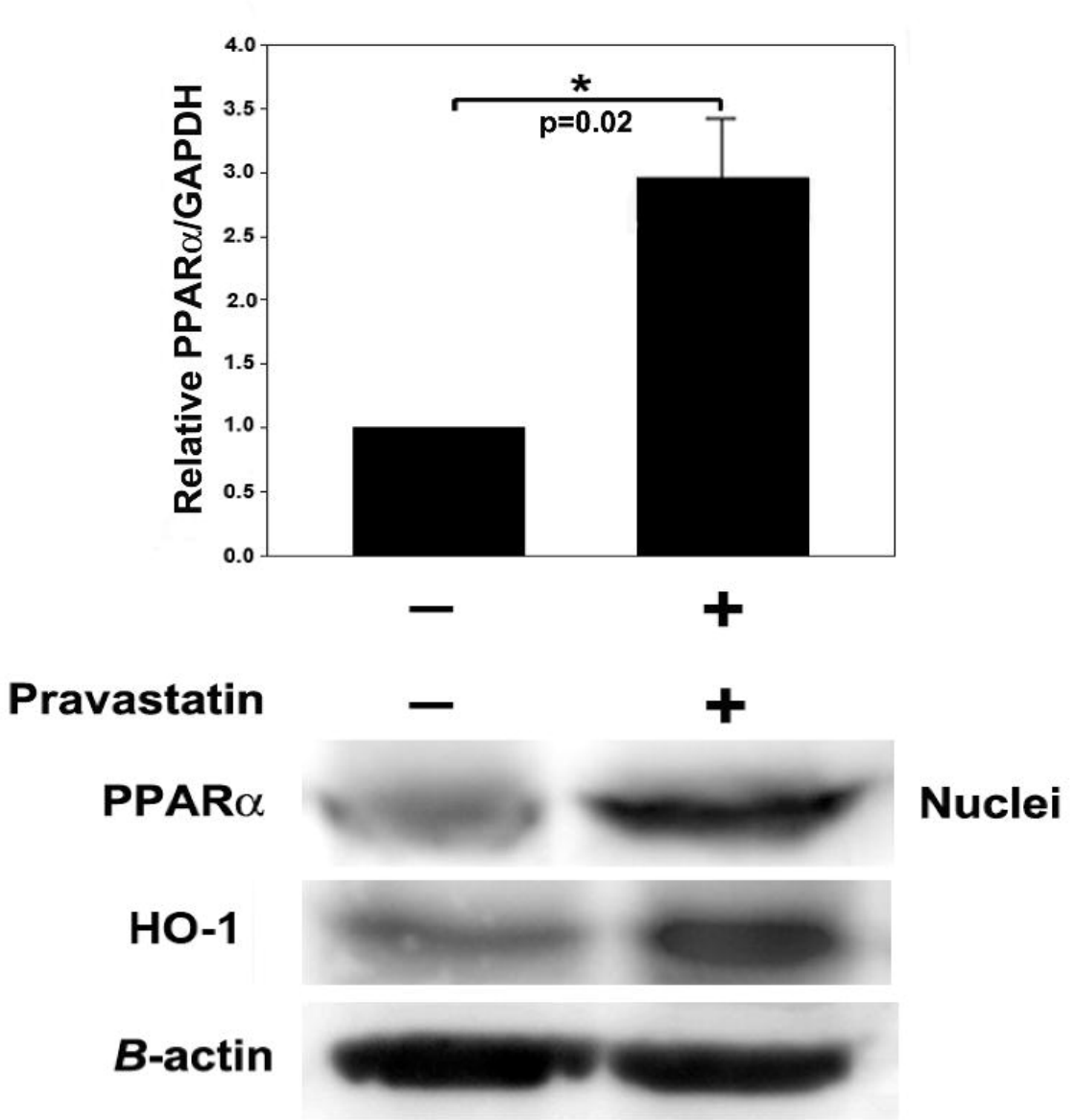
Relative PPARα/GAPDH
4.0
3.5
3.0
2.5
2.0
1.5
1.0
0.5
0.0
*
p=0.02
−
+
Pravastatin
−
+
PPARα
Nuclei
HO-1
B-actin

(B)

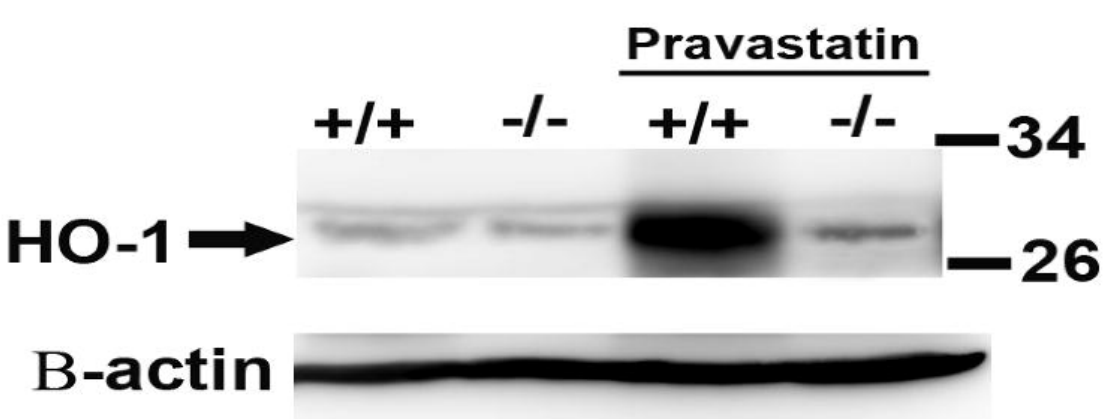
Pravastatin
+/+
-/-
+/+
-/-
34
26
HO-1
B-actin